Apparatus for high-resolution surface tension measurement

J. H. Magerlein[a] and T. M. Sanders, Jr.

Department of Physics, University of Michigan, Ann Arbor, Michigan 48104

(Received 1 November 1976; in final form, 12 July 1977)

We describe an apparatus for measuring surface tension of insulating liquids by capacitive sensing of capillary rise. Two guarded coaxial capacitors with different gap widths are connected to permit liquid to flow between them. The higher capillary rise in the narrow-gap capacitor is balanced by a dc voltage applied to the wide capacitor by a servosystem. In a measurement of the surface tension of liquid helium we obtain a resolution of 1 part in 10^5. The technique is well suited for automated measurements of small changes in surface tension.

I. INTRODUCTION

Many techniques have been used to measure surface and interfacial tension of liquids.[1] Capillary rise methods have potentially high resolution, although optical measurement of the meniscus position is often a limitation. For insulating liquids, resolution may be improved by allowing the liquid to rise between capacitor plates and deducing the height from the increase in capacitance.[2,3]

Since capillary rise must be measured with respect to the liquid height in some region of different gap, we find it advantageous to employ a pair of coaxial capacitors with different gap widths.[4,5] Surface tension causes liquid to rise higher in the narrow-gap capacitor. A capacitance bridge senses the height difference, and a dc balancing voltage is applied to draw liquid into the wide-gap capacitor until the levels are equalized. In this null-balance procedure the required dc voltage is a measure of the surface tension. Voltages may also be used to hold both liquid levels fixed as the liquid and gas densities change with temperature, thus minimizing the effects of capacitor surface irregularities.

Imperfections in our capacitors limit absolute accuracy to about 2% in measuring the surface tension of liquid helium near the superfluid transition temperature T_λ. We achieve a resolution of 1 part in 10^5 for changes in surface tension with temperature.

II. THE METHOD

Our differential capillary rise apparatus employs two coaxial capacitors designated C_w and C_n. The capacitors are equal in height, but C_w is larger both in diameter and gap. The capacitors are connected in a bridge, which measures the ratio C_w/C_n. For ideal capacitors this ratio does not change when the empty capacitors [Fig. 1(a)] are filled with any homogeneous dielectric [Fig. 1(b)]. It remains unchanged if a liquid of dielectric constant ϵ_l fills each capacitor to a height h and a gas of dielectric constant ϵ_g fills the remainder [Fig 1(c)].

The capacitors are joined to permit liquid to flow between them, and the bridge is balanced with the cell evacuated. Admitting liquid unbalances the bridge because the capillary rise is greater in C_n than in C_w. Balance is restored by drawing liquid into C_w with a dc voltage applied to that capacitor. An automatic null-balance system shown in Fig. 2 raises or lowers this voltage until the bridge is returned to balance and the liquid heights are equalized. The surface tension is calculated from the dc voltage required for balance.

Although the servosystem equalizes the two liquid heights, they will rise and fall together if the liquid and gas densities change. This might occur if surface tension is measured as a function of temperature. Such movement causes the meniscus to explore surface irregularities in the capacitors. We can minimize this source of error by applying a suitable dc voltage to C_n to draw liquid from a reservoir and fix the meniscus positions.

To relate the balancing voltages to the surface tension σ, we first calculate the height of the meniscus in a single capacitor relative to an infinite bath. We assume a geometrically ideal capacitor with a gap δ much smaller than its radius R so we may calculate the rise in a parallel-plate capacitor of gap δ and length equal to the perimeter $P = 2\pi R$. Some deviations from perfect capacitors are discussed later. We further assume that the capillary rise is large compared to δ so that the meniscus is circular. We write the condition for mechanical equilibrium by equating the gravitational force F_g to the sum of the surface tension force F_s and the electrostatic force F_e,

$$F_g = F_s + F_e. \tag{1}$$

The gravitational force is the weight of the liquid raised above the bath level minus the weight of the displaced gas. If the liquid volume above the bath level is V_l, we obtain

$$F_g = \Delta\rho g V_l = \Delta\rho g P h \delta,$$

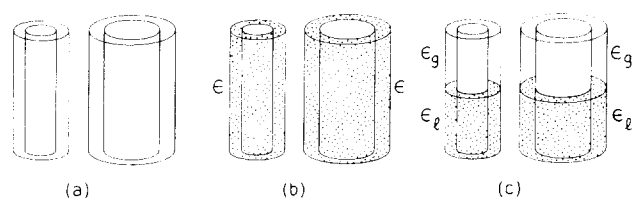

FIG. 1. Wide-gap and narrow-gap capacitors: (a) empty; (b) full of liquid; (c) filled to equal heights.

 0034-6748/78/4901-0094$00.60

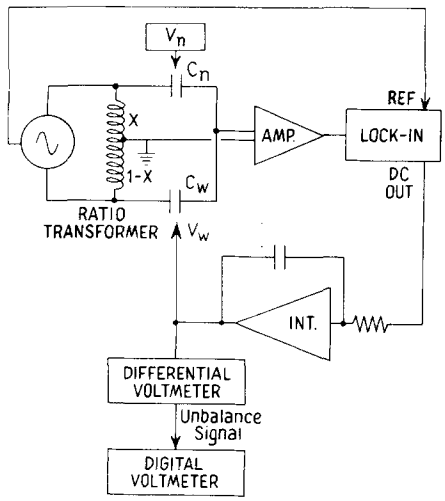

FIG. 2. Block diagram of instrumentation for surface tension measurement. The ratio transformer bridge detects changes in the ratio of the two cell capacitances C_n and C_w, and a feedback system adjusts V_w to keep the ratio constant.

where $h \equiv V_l/P\delta$ is an average liquid height and $\Delta\rho \equiv \rho_l - \rho_g$ is the difference between the liquid and gas densities. The total surface tension force at the two walls is

$$F_s = 2P\sigma \cos\theta,$$

where θ is the contact angle of the meniscus at the wall. The electrostatic force on a dielectric near conductors at constant potential can be written in terms of the change in electrostatic energy for a virtual meniscus displacement[6]

$$F_e = \frac{d}{dh}(\tfrac{1}{2}CV^2) = \frac{V^2}{2}\frac{dC}{dh}. \tag{2}$$

We may obtain the capacitance C from the energy relation

$$\tfrac{1}{2}CV^2 = (\epsilon_0/2)\int \epsilon E^2 dv.$$

Since errors in the field E produce only second-order errors in the energy, we may to lowest order in $(\epsilon_l - \epsilon_g)$ use the unperturbed constant field and take it outside the integral. To this order the capacitance depends simply on the average meniscus height h defined previously relative to the height h_0 of the bottom of the capacitor,

$$C = \frac{\epsilon_0 P}{\delta}\{\epsilon_l(h - h_0) + \epsilon_g[H - (h - h_0)]\}$$

$$= \frac{\epsilon_0 P}{\delta}[\Delta\epsilon(h - h_0) + \epsilon_g H], \tag{3}$$

where $\Delta\epsilon \equiv \epsilon_l - \epsilon_g$ is the difference of the liquid and gas dielectric constants and H is the total capacitor height. Using Eq. (2) we obtain

$$F_e = \epsilon_0 \Delta\epsilon V^2 P/2\delta.$$

This equation is valid for any fixed meniscus shape. Substituting into Eq. (1) yields the meniscus height

$$h = \frac{2\sigma\cos\theta}{\Delta\rho g\delta} + \frac{\epsilon_0\Delta\epsilon V^2}{2\Delta\rho g\delta^2}. \tag{4}$$

We now consider two capacitors C_w and C_n which in vacuum have a ratio C_{w0}/C_{n0}. With liquid in the cell, the voltages V_w and V_n are adjusted to restore this ratio. We see from Eq. (3) that this equalizes the two average heights h_w and h_n. Writing these heights from Eq. (4) yields

$$\sigma\cos\theta = \frac{\epsilon_0\Delta\epsilon}{4}\frac{V_w^2 - D^2V_n^2}{\delta_w(D-1)}, \tag{5}$$

where $D \equiv \delta_w/\delta_n$. For perfect capacitors, Eq. (5) gives the surface tension in terms of the applied voltages, the capacitor dimensions, and the dielectric constants. We use the gap ratio D because it can be measured directly to greater accuracy than the individual gaps. The capacitor dimensions D and δ_w are determined by electrical measurements as described in Sec. V below.

III. INSTRUMENTATION

We require a stable capacitance bridge which measures only the capacitance across the gap containing the liquid and gas. The ratio transformer bridge, shown schematically in Fig. 3, fulfills these requirements. The ratio transformer produces two ac voltages with a known amplitude ratio and with low source impedances. The balance condition for this idealized bridge is

$$\frac{e_n}{e_w} = \frac{Z_n}{Z_w} = \frac{C_w}{C_n}.$$

The performance of the bridge is limited only by the stability of the voltage ratio and by detector noise. Capacitance to ground on either side of the unknown capacitors does not affect the balance point. Capacitance from the high-level leads to ground merely appears across the zero-impedance generators. On the low-level

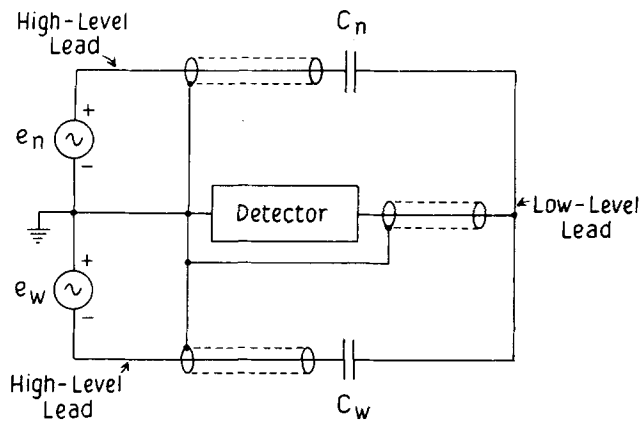

FIG. 3. Simplified ratio transformer bridge for guarded capacitance measurement. The ratio transformer is represented as two ideal voltage sources.

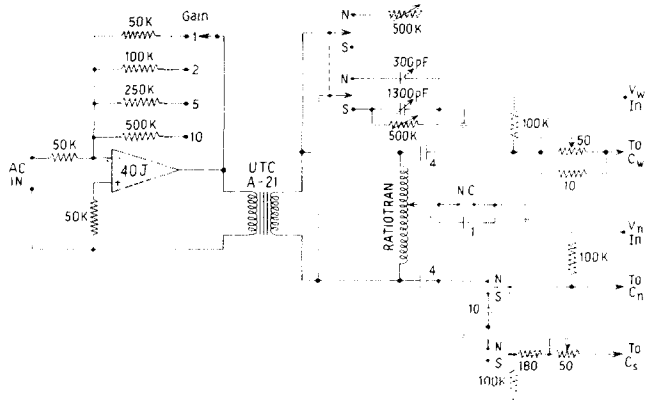

FIG. 4. Complete ratio transformer bridge. In the N switch position, the ratio of C_w to C_n is measured; in the S position, C_w is measured relative to C_s, the standard capacitor. Components to adjust the resistive bridge balance and to null the ratio transformer tap current are shown. The side of the bridge to which these must be connected depends on the cell capacitances and losses. Resistances are in ohms and capacitances in microfarads. The operational amplifier is made by Analog Devices, Inc., Norwood, MA.

side, capacitance to ground appears shunted across the null detector input, where it degrades the signal-to-noise ratio but does not shift the null. To measure only the desired capacitance, it is necessary to enclose all low-level parts entirely by a grounded shield or guard except at the measuring gap. This requirement must be kept in mind when designing the experimental cell.

The complete capacitance bridge circuit is shown in Fig. 4. The ratio transformer drive signal is supplied by a buffer amplifier and an isolation transformer. The bridge is driven at the resonant frequency of the null detector input circuit, about 9.3 kHz, with an amplitude of 1.7 V rms. The ratio transformer is a Singer[7] model 1011R precision ratio standard with a least count of 1×10^{-7} and an absolute accuracy of 1×10^{-6}. If the ratio transformer setting at balance is x, giving a voltage between the tap and the end terminal connected to C_n of x times the input voltage, the capacitance ratio is

$$C_w/C_n = x/(1 - x).$$

The drive signal is applied to the high-level capacitor plates through 4-μF coupling capacitors to block the dc balancing voltages. The dc voltages are applied through isolation resistors to avoid loading the ac voltage sources. The coupling capacitors and resistors must be large to avoid introducing errors into the bridge, but not so large that the RC time constant interferes with the servoloop stability. A low-inductance composition potentiometer is used in series with one capacitor to balance the dissipation in the two bridge arms.

To permit measuring the absolute capacitances C_w and C_n, a switch is provided to replace C_n in the bridge by a 100-pF standard capacitor, General Radio type 1404B. The ratio of C_w to the standard capacitor can be measured with the dc balancing voltages applied to the cell capacitors.

The ratio transformer does not, of course, have zero output impedance, particularly at our high operating frequency. Changes in output impedance with ratio setting are evidenced by unequal unbalance signal increments as the least significant ratio digit is advanced step by step. We minimize the effect of finite output impedance by nulling the current into the ratio transformer tap with 500-kΩ potentiometers and variable capacitors connected from the transformer ends to the tap. The current is correctly nulled when introducing additional impedance into the tap lead does not shift the null. A 1-μF capacitor is switched in for this purpose. After nulling the tap current, no further effects of ratio transformer output impedance are observed.

The capacitance bridge preamplifier employs an Analog Devices model 40J operational amplifier operated in the noninverting configuration with a closed-loop gain of 21. Lower voltage noise than the 7 nV/(Hz)$^{1/2}$ exhibited by this amplifier can be achieved by using discrete field-effect transistors.[8] This is not necessary here, since the amplifier voltage noise is not dominant.

Capacitance from the preamplifier input to ground should be minimized. In our apparatus the largest contribution is about 1000 pF between the cell active and guard sections. To minimize the signal loss caused by this parasitic capacitance, we resonate the total input capacitance with an inductor shunted across the amplifier input. This increases the signal voltage at the amplifier input by approximately the Q of the resonant circuit. The noise is also increased. Losses in the inductor introduce Johnson noise, and the higher source impedance increases the effect of amplifier current noise. The total input noise voltage E_n is

$$E_n = B^{1/2}[e_n^2 + 4kTQ/\omega C_T + (i_n Q/\omega C_T)^2]^{1/2},$$

where B is the detector bandwidth, e_n^2 and i_n^2 are the mean square amplifier voltage and current noise per unit bandwidth, respectively, at the operating frequency ω, T is the inductor temperature, and C_T is the total amplifier input capacitance. The signal for a change ΔC in one of two equal capacitors C in the bridge is

$$E_s = e_g \Delta C Q/C_T,$$

where e_g is the bridge driving voltage. The minimum detectable $\Delta C/C$ for a signal-to-noise ratio of one is

$$\left(\frac{\Delta C}{C}\right)_{\min} = \frac{C_T B^{1/2}}{C e_g}\left[\frac{e_n^2}{Q^2} + \frac{4kT}{\omega C_T Q} + \left(\frac{i_n}{\omega C_T}\right)^2\right]^{1/2}.$$

For $B = 1$ Hz, $C_T = 1000$ pF, $C = 50$ pF, $e_g = 1.7$ V, $e_n = 7$ nV Hz$^{-1/2}$, $i_n = 2 \times 10^{-14}$ A Hz$^{-1/2}$, $Q = 50$, $T = 300$ K, and $f = \omega/2\pi = 10$ kHz, the fractional capacitance resolution is 3×10^{-8}. Since the Johnson noise term dominates, cooling the inductor would reduce electronic noise. This is unnecessary here, since ripples on the liquid surface produce noise comparable to the electronic noise.

The resonant circuit at the preamplifier input also rejects signals far from the bridge excitation frequency. This permits using a broadband lock-in amplifier, the Princeton Applied Research model 128A, as the

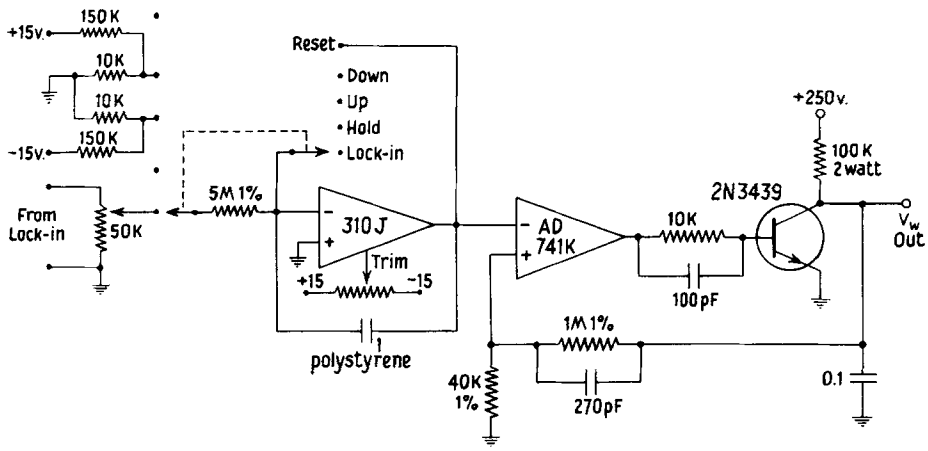

FIG. 5. Integrator and high-voltage amplifier. The five-position switch opens and closes the servoloop and permits manual adjustment of the balancing voltage. The operational amplifiers are made by Analog Devices, Inc. Except as marked, resistances are in ohms and capacitances in microfarads.

detector. The lock-in gain is set to the highest value consistent with good servoloop transient response. Since excessive low-pass filtering can cause loop instability, we use a single-section filter with a time constant of 0.1 s or less.

The detector output is integrated and amplified by the circuit shown in Fig. 5 to produce a balancing voltage V_w of about 200 V. The integrator makes this a true null-balance system. With the capacitance bridge exactly at null, the integrator maintains the proper balancing voltage. Without the integrator the capacitance bridge would remain slightly off balance due to finite loop gain. It is convenient to open the servoloop at the integrator input while measuring capacitor gaps and adjusting V_n. The voltage V_w must remain constant during these operations, so it is necessary to use an integrating capacitor with low leakage and dielectric absorption and an amplifier with extremely low bias current. Using a 1-μF polystyrene capacitor and a varactor bridge amplifier with a bias current of 1×10^{-14} A, the voltage is constant within 1 part in 10^5 for at least 5 min.

We measure the dc balancing voltage using a Fluke model 895A differential voltmeter with a specified stability of 8 parts in 10^6 per day. To achieve the rated accuracy, the meter is operated within 0.1 V of null. A digital panel meter reads the unbalance signal. The dc voltage applied to the narrow capacitor ranges from zero to about 70 V in our experiment and is measured with a Fluke model 881A differential voltmeter. Since V_n is smaller than V_w, it does not need to be measured as accurately.

IV. EXPERIMENTAL CELL

The surface tension cell containing the coaxial capacitors is illustrated in Fig. 6. The capacitors are arranged concentrically; this design is less sensitive to tipping than one with side-by-side capacitors. The two capacitors share a common low-level electrode, which is part of a hollow cylindrical assembly also containing two grounded guard sections and two end sections for positioning. The different sections are attached with insulating epoxy joints. The two high-level capacitor plates are the cylinders located inside and outside of this assembly. The inner cylinder also has insulated end sections for positioning. An additional gap at the outside serves as a reservoir which permits us to hold the levels in both measuring gaps fixed as the liquid and gas densities change with temperature. This gap also eliminates pressure differences across the critical capacitor walls to minimize distortion from internal cell pressure. The three gaps are joined both in the liquid and the gas phases.

Our cell is constructed from copper for high thermal conductivity at low temperatures. The four demountable assemblies are positioned and centered by press-fit joints and are sealed together with indium wire gaskets. Stycast 2850FT epoxy[9] provides an insulating bond between the parts of the multisection assemblies and seals the lead wires. Contact to the active section is made through the center conductor of a coaxial cable with a solid copper shield.[10] The shield contacts the upper guard section; the lower guard connection comes out the bottom of the cell through a connector.

Our narrow and wide capacitors have average diameters of about 18.9 and 31.6 mm and gaps of approxi-

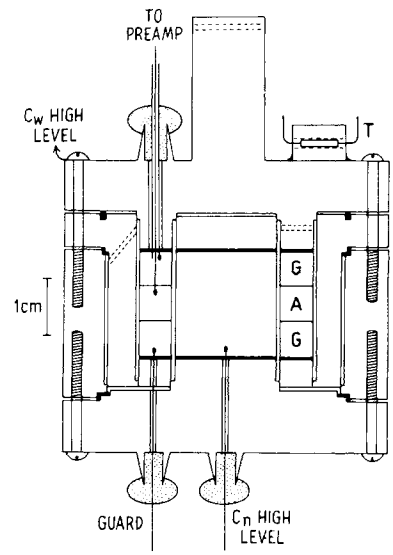

FIG. 6. Surface tension cell. The active section A is between the two guard sections G. A thermometer T is mounted on the cell. There are four separate parts, sealed together with indium wire gaskets. Each of the inner two assemblies consists of several sections epoxied together.

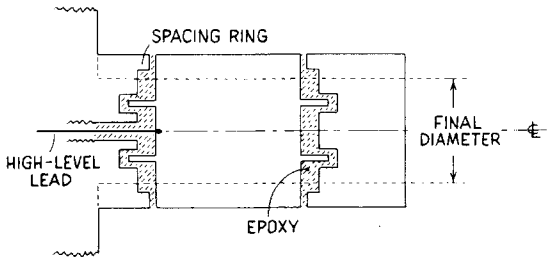

FIG. 7. Construction of cell inner cylinder. The spacing ring, which is machined off after the epoxy hardens, assures correct spacing of the sections.

mately 0.069 and 0.081 mm. The empty capacitances are about 48 and 68 pF. Optimum capacitor dimensions depend on the magnitude of the surface tension to be measured, the maximum balancing voltage which can be sustained without breakdown, thermal contact requirements, and convenience of construction. The indium gaskets and Stycast epoxy seals are appropriate in our low-temperature environment; other applications may suggest different techniques. The cell may need to be constructed of a material with a low thermal expansion coefficient if it is to be used at higher temperatures.

The multisection assemblies are constructed as illustrated in Fig. 7. Each disk is originally made larger in outside diameter than the finished dimension. A narrow ridge around the outside of one face acts as a spacer to ensure an epoxy layer of the correct thickness. The active section is separated from the guard disks by about 0.015 mm of epoxy. The insulators adjoining the locating sections are wider, about 0.2 mm, since they must withstand the dc balancing voltages.

The sections are epoxied together one by one, and the whole assembly is turned down to the final diameter. We use carbide lathe tools, but even these are rapidly dulled by the alumina-loaded Stycast epoxy. The machining process pushes some of the soft copper into the epoxy gaps and produces short circuits between sections. A brief electropolish primarily attacks the high-field areas along the gaps and removes the short circuits. The parts are polished with a series of alumina abrasives and electroplated with gold. The polished surfaces have a shiny appearance, but examination with a magnifying glass reveals many pits and scratches up to about 10 μm in size.

V. PROCEDURE

We have used two different experimental procedures. One is readily automated; the other is more complicated but yields greater resolution. Sample data are shown below for both procedures. The simpler method uses no dc voltage on C_n; the surface tension is obtained by measuring the voltage V_w required to keep the capacitance bridge at balance. In our experiment we cause the cell temperature to drift and record a thermometer resistance and a value of V_w at regular temperature intervals. We automated the measurement under the control of a digital data-logging interface.[8]

This procedure did not yield sufficient resolution for our purposes because of irregularities in the capacitor surfaces. Although the servosystem keeps the liquid levels in the capacitors equal, the two levels move up and down over the imperfections as the liquid and vapor densities change with temperature. Particularly severe irregularities produce jumps in the balancing voltage as large as 0.1 V, after which the voltage continues with its previous slope. On reversing the temperature drift, a similar jump in the other direction is seen. We observe some hysteresis, as would be expected if the liquid sticks at an irregularity. We avoid taking data at filling levels which show these large discontinuities, but smaller irregularities still can distort the data.

These effects can be reduced by holding the liquid levels fixed in both capacitors at all temperatures. As before, V_w is adjusted by the servo to equalize the levels in the two capacitors. In addition, a voltage V_n across the narrow capacitor is adjusted manually to keep the absolute heights fixed. This procedure requires measuring the value of one of the cell capacitors as well as the ratio. For this purpose we measure the ratio of C_w to the 100-pF standard capacitor. If the dielectric constants of the two phases are known as functions of temperature, the capacitance C_w required to maintain a constant filling level can be calculated. Since adjusting either voltage changes both capacitances, V_n and V_w must be adjusted iteratively until both C_w and the ratio C_w/C_n converge to their desired values. This procedure is more difficult to automate, and we take data manually point by point.

The capacitor gaps, which must be known to calculate the surface tension, may be determined by capacitance measurements. The gap ratio $D = \delta_w/\delta_n$ is measured at the filling level used to measure surface tension. First we measure C_w at some temperature with a combination of V_n and V_w which balances the bridge. Material is added to or removed from the cell, and V_n and V_w are adjusted to new values V_n' and V_w' until both C_w and the ratio C_w/C_n return to their original values. This ensures that the liquid levels in both capacitors are unchanged. Only the reservoir level is different. To obtain D, we equate the surface tension values from Eq. (5) before and after changing the amount of liquid, and obtain the result

$$D = [(V_w^2 - V_w'^2)/(V_n^2 - V_n'^2)]^{1/2}.$$

We must also measure the wide capacitor gap δ_w. For an ideal capacitor of perimeter P and height H, the gap can be determined by a single measurement of the empty capacitance C_0,

$$\bar{\delta} = \epsilon_0 PH/C_0. \tag{6}$$

For our imperfect capacitor, we must evaluate the gap at the meniscus. We first balance the bridge at the vacuum ratio x with known voltages V_w and V_n. A small change Δx is made in x, and the voltage on the capacitor being measured is adjusted to rebalance the

bridge. The other voltage is held constant. The resulting value of $(\Delta V^2)/\Delta x$ is used to calculate the gap.

The calculation is simple if the gaps are constant over the range the meniscus moves during the measurement, even if large variations exist elsewhere in the capacitor. Using the conservation of matter along with Eq. (4) yields the expression for δ_w at the surface,

$$\delta_w = \left[\frac{\epsilon_0^2(\Delta\epsilon)^2 x(1-x)P_w}{2\Delta\rho g C_w} \frac{d(V_w^2)}{dx} \right]^{1/3} \times \left[1 + \frac{A_w}{A_T} \left(\frac{\bar{\delta}_n \delta_w}{\bar{\delta}_w \delta_n} - 1 \right) \right]^{1/3}, \quad (7)$$

where A_w is the cross sectional area of the wide gap at the surface, A_T is the total of the narrow, wide, and reservoir gap areas, and $\bar{\delta}_n$ and $\bar{\delta}_w$ are the average gaps given by Eq. (6). The second term in Eq. (7) is within 0.5% of unity for our reasonably uniform capacitors. A similar expression may be derived for δ_n in terms of $d(V_n^2)/dx$.

We calculate the gaps more accurately by assuming a linear variation in the gap of each capacitor over the region the meniscus moves during the measurement. The amount of the taper is determined by fitting a line through gap measurements taken over a 3-mm length. We calculate corrections to Eq. (7), which change the gap values by about 3% for the tapers found in our cell. Scatter in the gap measurements, however, indicates a surface roughness which may invalidate such a correction procedure based on linear tapers.

VI. PERFORMANCE

We measured the surface tension of liquid helium over a temperature range of about 100 mK on either side of T_λ. The surface tension is calculated from the balancing voltages using Eq. (5); for the data with constant liquid levels, two weakly temperature-dependent corrections described below are applied. Due to the presence of the helium film, the liquid wets the capacitor plates perfectly, and the contact angle θ is taken to be zero. The gap ratio D and the wide gap δ_w are calculated from measurements described previously. Measurements of the helium liquid dielectric constant[11] and the vapor density[12] give $\Delta\epsilon$ within 1 part in 10^5.

Surface tension data taken with the temperature drifting and $V_n = 0$ are shown in Fig. 8 for two different filling levels in the cell. A linear background has been subtracted from the data. The surface tension is plotted against the reduced temperature $t \equiv (T - T_\lambda)/T_\lambda$ with one data set displaced upward for clarity. The irregularities in the curves and most of the disagreement between the data sets result from imperfections in the capacitor surfaces. The "waves" apparently reflect regular surface features left from machining or polishing. If errors of such a magnitude are acceptable, this method of taking data is simple and easily automated.

The data of Fig. 9 are taken point by point using V_n to hold the liquid levels fixed at all temperatures.

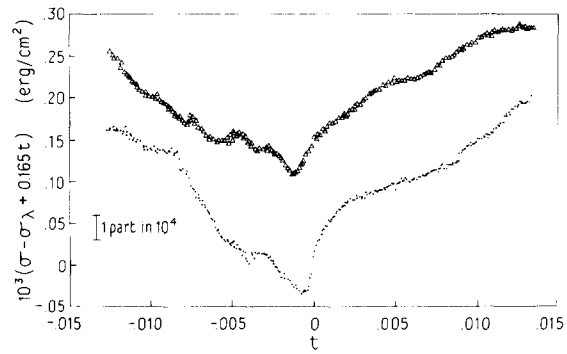

FIG. 8. Surface tension of liquid ^{4}He minus a straight line plotted against reduced temperature $t \equiv (T - T_\lambda)/T_\lambda$. The data are taken automatically with the temperature drifting and $V_n = 0$. The dots and triangles are data at two different filling levels, with the latter displaced upward by 0.15×10^{-3} erg/cm².

To see random scatter in the data we display the central region on an expanded scale in Fig. 10. Random noise and drift over a period of several days limit resolution at about 1 part in 10^5. For our capacitor geometry and the dielectric constants of helium gas and liquid, this corresponds to a capacitance resolution of about 1 part in 10^7 and a height resolution of about 10 nm.

Systematic errors are much larger than the random errors described above. The most serious ones result from uncertainties in the capacitor gap parameters. The uncertainty in δ_w, which appears as a multiplicative error in σ, is about 1% in our cell. The gap ratio D is measured with an uncertainty of about 0.1% at the fillings used to take data. An error in D will distort the data in a manner which depends on the values of V_n which are required to hold the liquid levels constant.

The two previous errors result from uncertainties in the gap values at the liquid surface. Deviation of the capacitors from perfect cylinders anywhere in the active section can also introduce surface tension errors. In deriving our expression for the surface tension, we used the condition $h_w = h_n$, although we actually maintain the capacitance ratio C_w/C_n at its vacuum value. For imperfect capacitors, this condition does not imply equality of heights, leading to a weakly temperature-dependent additive correction to the surface tension. For a given height difference $\Delta h \equiv h_n - h_w$, the equation for the surface tension becomes

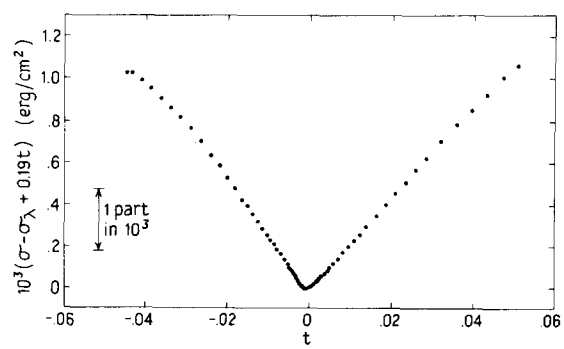

FIG. 9. Surface tension data taken point by point using V_n to hold the liquid levels constant.

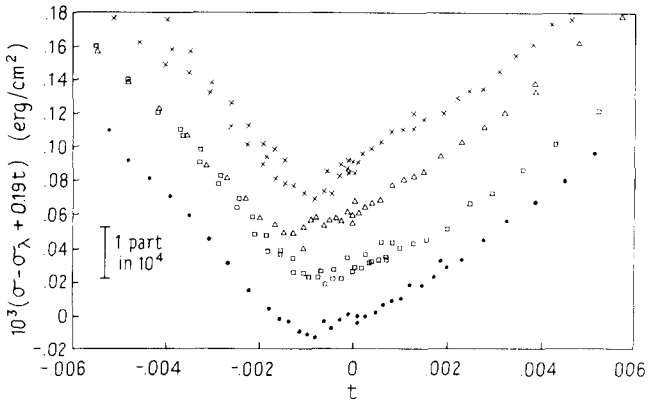

FIG. 10. Expanded view of data near T_λ. The different symbols indicate data at four different filling levels, displaced successively upward by 3×10^{-5} erg/cm^2.

$$\sigma = \frac{\epsilon_0 \Delta\epsilon}{4} \frac{V_w^2 - D^2 V_n^2}{\delta_w (D-1)} + \frac{\Delta\rho g \delta_w}{2(D-1)} \Delta h. \qquad (8)$$

A calculation of the height difference Δh requires knowledge of the entire profile of the capacitors. Fortunately, the temperature dependence of the correction is quite weak (it has approximately the temperature dependence of $\Delta\rho$), so this effect produces nearly a simple additive correction to the surface tension. We observe additive shifts between data sets at different fillings (σ at T_λ varied from 0.312 to 0.324 erg/cm^2) consistent with observed variations in gap near the ends of the capacitors. A correction of the form of Eq. (8) is applied to each set with Δh chosen to normalize $\sigma(T_\lambda)$ to 0.307 erg/cm^2.[13] Such a normalization method produces far better agreement between sets than applying a multiplicative correction.

Other systematic errors amount to less than 2 or 3 parts in 10^5 in our experiment.[5] Stray capacitance with dielectrics other than helium, which can cause inequality of the liquid heights at balance, is held to about 3×10^{-3} pF by careful guarding. Distortion of the cell with changes in temperature, internal pressure, or electric field can be detected by measuring the capacitance ratio with the cell full of liquid. These distortions are minimized in our experiment by the small coefficient of expansion of materials at our low operating temperature and the relatively low vapor pressure of helium near T_λ. A small correction for cell distortion with pressure has been applied to our data. The bridge excitation voltage also affects the balance condition; its effect could be neglected in our experiment. Remaining effects of surface irregularities can be estimated by comparing data at different filling levels.

VII. IMPROVEMENTS

Further improvement in accuracy and resolution depends largely on smoother capacitor surfaces and more uniform gap widths. Improved capacitors could reduce systematic errors and perhaps eliminate the need to keep the liquid levels fixed. Materials other than copper may be superior if high thermal conductivity is not needed. Gold plated quartz plates[3] have an excellent surface finish, but edge irregularities may be troublesome and it may be difficult to maintain proper guarding. Stability of the cell capacitors may be more difficult to achieve in other environments. The limitation imposed by ripples on the liquid surface might be overcome by more careful vibration isolation. The capacitance resolution can easily be improved by better preamplifier design if this is warranted. At the present level of resolution, this technique has proved valuable for measuring the weak singularity in the surface tension of liquid helium near T_λ.

ACKNOWLEDGMENT

Work supported in part by the National Science Foundation.

[a] Present address: IBM Thomas J. Watson Research Center, Yorktown Hts., NY 10598.

[1] N. K. Adam, *The Physics and Chemistry of Surfaces* (Oxford U. P., London, 1941), 3rd ed.; J. T. Davies and E. K. Rideal, *Interfacial Phenomena* (Academic, New York, 1963), 2nd ed.
[2] D. P. E. Dickson, D. Caroline, and E. Mendoza, Phys. Lett. A **33**, 139 (1970).
[3] F. M. Gasparini, J. Eckardt, D. O. Edwards, and S. Y. Shen, J. Low Temp. Phys. **13**, 437 (1973); J. R. Eckardt, Ph.D. thesis (Ohio State University, 1973) (available from University Microfilms, Ann Arbor, MI).
[4] J. H. Magerlein and T. M. Sanders, Jr., Phys. Rev. Lett. **36**, 258 (1976).
[5] J. H. Magerlein, Ph.D. thesis (University of Michigan, 1975) (available from University Microfilms, Ann Arbor, MI).
[6] J. D. Jackson, *Classical Electrodynamics* (Wiley, New York, 1962), pp. 126–127.
[7] Singer Instrumentation, 3211 South La Cienega Blvd., Los Angeles, CA 90016.
[8] J. H. Magerlein and T. M. Sanders, Jr., Rev. Sci. Instrum. **46**, 1653 (1975).
[9] Emerson and Cuming, Canton, MA 02021.
[10] Type UT-20, Uniform Tubes, Collegeville, PA 19426.
[11] C. T. Van Degrift, Ph.D. thesis (University of California, Irvine, 1974) (available from University Microfilms, Ann Arbor, MI).
[12] W. E. Keller, Phys. Rev. **97**, 1 (1955).
[13] K. R. Atkins and Y. Narahara, Phys. Rev. A **138**, 437 (1965).